QUANTIFICATION OF MODELLED WIND TURBINE NOISE GROUND REFLECTIONS

Josephine Siebert Pockelé[1], Roberto Merino-Martinez[1], Mirjam Snellen[1]

[1] *Faculty of Aerospace Engineering, Delft University of Technology, the Netherlands*

This contribution has been accepted based on the submitted abstract. The submitted manuscript was not reviewed and is reproduced here without edits or corrections by the conference board. Neither the EAA nor the AAA take responsibility for its contents.

Abstract

Ground reflections play an important role in the propagation of wind turbine noise and significantly affect noise assessment. For simplicity, most best-practice wind turbine noise prediction models treat the entire wind turbine as a point source, typically located at the rotor hub. Nevertheless, leading-edge and trailing-edge noise (the main noise generation mechanisms in modern wind turbines) is better represented by a line source along each blade. This paper proposes a method for assessing ground reflections that accounts for the spanwise distribution of acoustic power by approximating it as multiple point sources. Results for a 5-MW reference wind turbine show that most acoustic interference occurs below 5 kHz. Moreover, loss of phase coherence due to atmospheric turbulence further reduces the acoustic interference. Using too few point sources in the distribution can lead to aliasing, thereby affecting the accuracy of blade-element-based wind turbine noise models. Overall, the proposed method estimates lower acoustic interference than common single-point-source models, suggesting that current prediction methodologies are likely overestimating the effect of ground reflections in their calculations, potentially leading to misleading results that may fail to match experimental data.

Keywords: *ground reflections, wind turbine noise, ground impedance, amplitude modulation*

1. Introduction

Conventional horizontal-axis wind turbines are among the main technologies that support the worldwide supply of sustainable energy. While recent technological advances primarily focus on offshore wind, the majority of new turbines in Europe are still installed onshore [1]. In the planning and permitting phase of onshore wind farms, noise emissions play an important role. On one hand, turbines must comply with various international noise regulations [2], while on the other hand, surrounding communities report experiencing noise annoyance [3].

Propagation effects for wind turbine noise are commonly modelled by assuming a single point source. While Tian and Cotté [4] show that this assumption has a limited effect on the overall sound pressure level, they demonstrate a significant overestimation of acoustic interference and amplitude modulation due to the ground effect. In auralisation, this can significantly affect the listener's perception. Therefore, this paper explores a method to determine the ground effect for wind turbine noise that accounts for a more realistic distribution of acoustic power along the blade span. This more closely mimics the main noise-generation mechanisms in modern wind turbines: leading-edge and trailing-edge noise. The proposed method targets applications where source information is available only per blade or for a full rotor, similar to the modelled auralisation approach in Pockelé and Merino-Martínez [5].

Section 2 presents the proposed method and the turbine geometry to which it is applied. Section 3 shows ground effect spectrograms for one blade and a three-bladed rotor, including short discussions about the IEC setup and the loss of phase coherence. Section 4 continues with a brief sensitivity analysis of the method, followed by a comparison to conventional point source methods in Section 5.

2. Methodology

This paper proposes a modelling approach which combines two methods: (1) the distribution of the total acoustic source energy over a line source represented by discrete point sources, and (2) the source-mirror model to determine the ground effect of the individual sources.

Corresponding author: *j.s.pockele@tudelft.nl.*

2.1. Distribution of source power

In this work, the total acoustic energy created by a wind turbine blade is distributed over N point sources, evenly spaced along the blade span. The relative sound power per source is approximated by

$$|p|^2 \sim M^5 \hat{c}^2 \delta \tag{1}$$

where M is the Mach number, $\hat{c}$ the chord length , and δ boundary layer thickness [6], [7]. The local Mach number at source n is

$$M_n = \frac{\sqrt{(\omega R_n)^2 + V_\infty^2}}{c} = \frac{\omega \sqrt{R_n^2 + (R/\lambda)^2}}{c} \tag{2}$$

where ω is the rotor speed, R_n the spanwise position of source n, V_∞ the free field wind speed, c the speed of sound, R the blade radius, and λ the tip-speed ratio. The boundary layer thickness is approximated as [8]

$$\delta_n \approx 0.376 \left(\frac{\rho\, \hat{c}_n M_n c}{\mu} \right)^{-1/5} \tag{3}$$

Finally, the discrete acoustic source power distribution, shown in Figure 1, is estimated with Equation 4.

$$\left| \frac{p_{n,0}}{p_0} \right|^2 = \frac{M_n^5 \cdot \hat{c}_n^2 \cdot \delta_n}{\sum_n \left(M_n^5 \cdot \hat{c}_n^2 \cdot \delta_n \right)} \tag{4}$$

where $p_{n,0}^2$ is the relative power of source n and p_0 is the overall source power of the full blade.
Sources located within the hub radius R_{hub} are not considered as this part of the rotor is not a relevant aeroacoustic source.

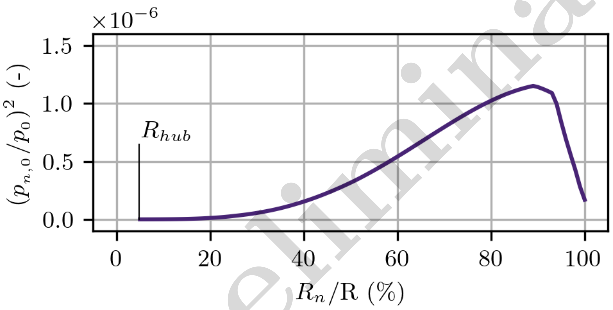

Figure 1: Distribution of source power over the blade of the NREL 5-MW reference wind turbine, using the parameters in Table 1 and $N = 101$ point sources.

2.2. Source-mirror ground effect model

The acoustic ground effect of a single source-receiver pair is modelled with the method by Embleton, Piercy, and Daigle [9]. The underlying source-mirror geometry is illustrated in Figure 2.
In this model, the received sound pressure, p, consists of the contribution from the direct propagation path r_1 and the reflected path r_2. For one source-receiver pair, the ratio between the received and source pressure at 1 m, p/p_0, is captured by Equation 5.

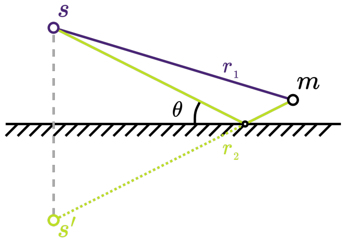

Figure 2: Geometry of the source-mirror ground reflection model. Source s, mirror source s', receiver m.

$$\frac{p}{p_0} = \frac{e^{ikr_1}}{r_1} + Q\,\frac{e^{ikr_2}}{r_2} \tag{5}$$

where the reflection coefficient Q accounts for the interaction between the reflected sound and the ground material.

$$Q = R_p + (1 - R_p)F \tag{6}$$

where R_p is the plane wave reflection coefficient, and F is the spherical wave loss factor. R_p is determined, assuming a locally reactive surface, using the ground impedance Z_n and grazing angle θ:

$$R_p = \frac{Z_n \sin(\theta) - 1}{Z_n \sin(\theta) + 1} \tag{7}$$

where Z_n is estimated through the single-parameter model by Delany and Bazley [10]:

$$Z_n = 1 + 9.08 \left(\frac{f}{\sigma_e} \right)^{-0.75} - 11.90i \left(\frac{f}{\sigma_e} \right)^{-0.73} \tag{8}$$

2.3. Total ground effect

The relative sound power of each source at the receiver, $|p_n/p_0|^2$, is estimated by scaling Equation 5 with Equation 9:

$$\left| \frac{p_n}{p_0} \right|^2 = \left| \frac{p_{n,0}}{p_0} \right|^2 \cdot \left| \frac{e^{ikr_{n,1}}}{r_{n,1}} + Q\,\frac{e^{ikr_{n,2}}}{r_{n,2}} \right|^2 \tag{9}$$

Using Equation 9, the total ground effect of a wind turbine blade, ΔSPL_G, is obtained by:

$$\Delta SPL_G = 10 \log_{10} \left\{ \frac{\sum_n |p_n/p_0|^2}{\sum_n |p_{n,0}/p_0|^2 / r_{n,1}^2} \right\} \tag{10}$$

where the denominator represents the propagation to the receiver without ground effect.
Equation 10 poses one limitation by its implicit assumption that all blades have an equal source power $|p_0|^2$ throughout the full rotation. Atmospheric gradients (e.g., wind, temperature) inherently cause time-varying source intensities that differ between blades. In practice, this would change the inter-blade interference patterns shown in the results.

2.4. Wind turbine geometry

The geometrical setup implemented for the proposed method is shown in Figure 3. This paper focuses on the NREL 5-MW reference wind turbine [11], whose relevant specifications are listed in Table 1.

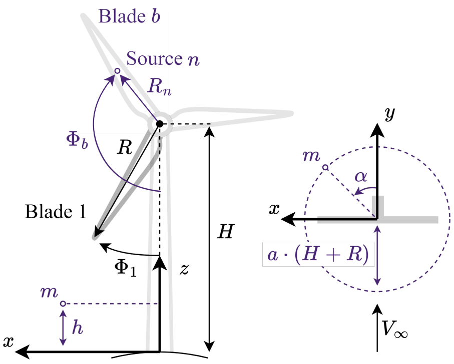

Figure 3: Wind turbine and geometry parameters.

Table 1: Relevant specifications of the NREL 5-MW reference wind turbine [11].

Rotor radius	R (m)	63.0
Hub radius	R_{hub} (m)	1.5
Hub height	H (m)	90.0
Rated rotor speed	ω (RPM)	12.1
Design tip speed ratio	λ (-)	8.0

3. Results

In this section, results from the proposed method are presented, using the parameters defined in Table 1. The ground material's flow resistivity is set equivalent to grass ($\sigma_e = 250$ kPa/m^{2}s). The receiver is located at IEC position 1 ($a = 1,\ \alpha = 0$; see Figure 3) and at a representative height for human perception ($h = 1.7$ m). The number of point sources N is set appropriately for each figure, so as to avoid the aliasing described in Section 4. The selected values of N are reported in the captions. Each spectrogram covers a full rotor rotation ($\Phi_1 : 0 \rightarrow 2\pi$; see Figure 3).

Figure 4 shows spectrograms of the acoustic ground effect of one turbine blade. Above 5 kHz, this model shows little to no interference, with sound amplifications mostly constant between 0 dB and 1 dB. Therefore, the remainder of this paper focuses on the results in the 0-5 kHz range. Two blade angles are identified where the interference covers the full frequency spectrum. These correspond to a geometry where the grazing angles θ_n of all sources are approximately equal. The interference patterns in Figure 4 result from the alignment between the interference patterns of the individual sources, rather than acoustic interference between these sources. At lower frequencies, the longer wavelengths lead to more alignment across blade azimuth angles, Φ_1, thereby increasing the duration of the interference.

Figure 5 shows the acoustic ground effect caused by a full three-bladed wind turbine rotor. Compared to a

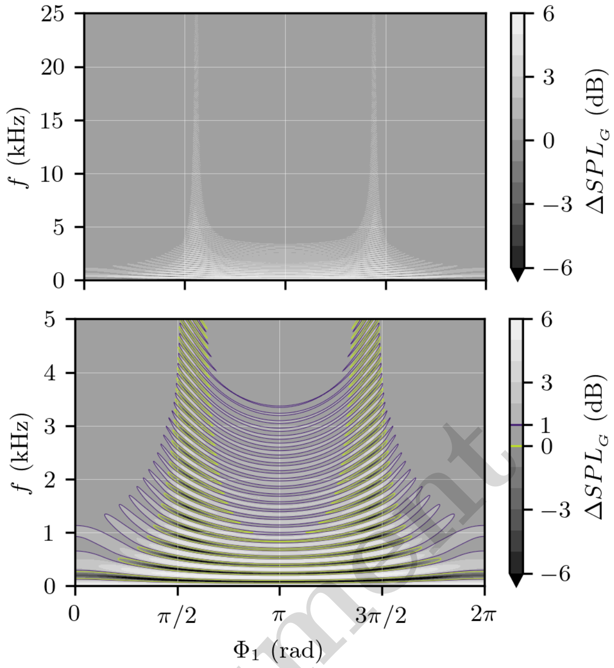

Figure 4: Acoustic ground effect from a single wind turbine blade during a full rotor rotation, for the full spectrum (top, $N = 1001$) and zoomed-in version (bottom, $N = 101$).

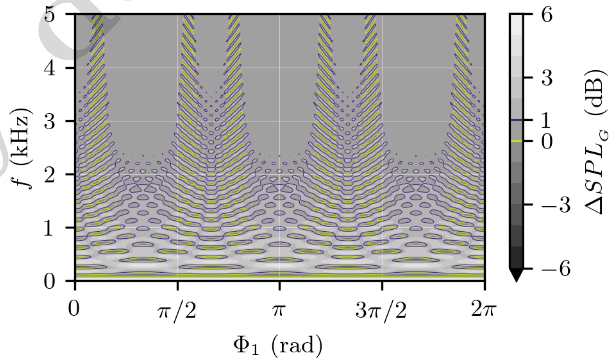

Figure 5: Acoustic ground effect from a three-bladed wind turbine rotor during a full rotor rotation ($N = 3 \times 101$).

single blade, these results show less interference due to the additional interaction between the three blades. Similar to the result for one blade, most of the spectrogram at high frequencies shows a limited amplification of 0-1 dB, interrupted by a short-duration interference pattern.

3.1. Phase coherence loss

This modelling approach implicitly assumes the direct and reflected signals remain fully coherent. However, sound propagation through a turbulent atmosphere can cause partial loss of phase coherence between the two signals, reducing interference. In case of full coherence loss, the ground effect of a point source converges to a frequency-dependent amplification without interference [12]. Figure 6 shows this effect on the results

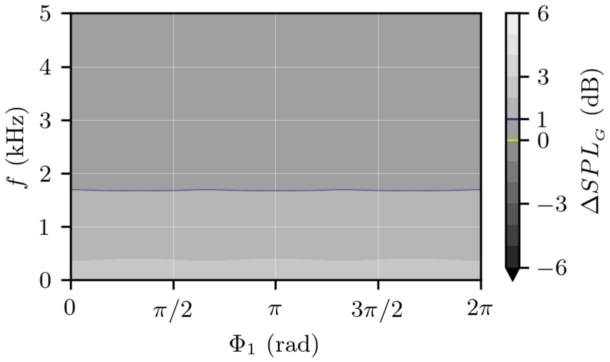

Figure 6: Acoustic ground effect from a three-bladed wind turbine rotor during a full rotor rotation, with full loss of phase coherence ($N = 101$).

for a three-bladed rotor. Above 2 kHz, an amplification of 0-1 dB is observed, while the amplification at lower frequencies is up to 3 dB. Coherence losses are expected to primarily affect results at higher frequencies, however. While a complete loss of phase coherence is unlikely, it is still worth considering to understand how coherence loss may affect ground reflections.

3.2. IEC setup

The IEC standard for wind turbine noise measurements [13] prescribes a microphone mounted to a circular, highly reflective plate, directly on the ground. The post-processing steps then assume a constant 6 dB amplification from the resulting reflections. Figure 7 shows the result from the presented model, at a receiver height of 1 mm, with $\sigma_e = 10^7$ kPa/m^2·s to represent the standardised setup. The spectrogram shows a nearly constant amplification between 5.6 dB and 6.0 dB, confirming the IEC standard's assumption.

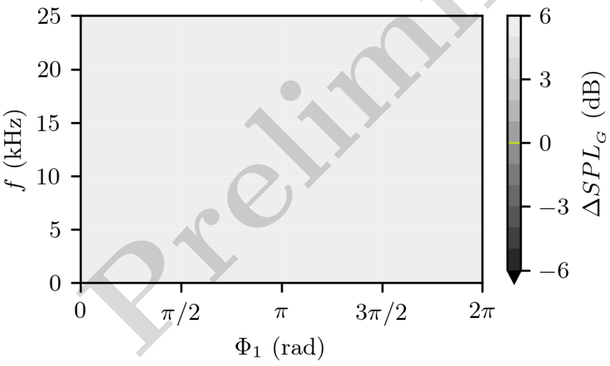

Figure 7: Acoustic ground effect determined for the IEC standardised measurement setup [13] ($N = 101$).

4. Sensitivity analysis

This section briefly investigates how the flow resistivity σ_e and the number of point sources N affect the acoustic ground effect.

The effect of σ_e on the results is presented in Figure 8. The main observation is an increase in acoustic amplification with increasing flow resistivity. This is especially evident from the area with little interference, where the amplification increases from a 0-1 dB range to a 2-4 dB range. The interference in this area is also increased slightly, as evidenced by the increasingly visible fringes in Figure 8b and 8c. Less evident is the increased interference at lower frequencies and at the previously highlighted asymptotic blade angles, which is expected given the increasing ground surface reflectivity.

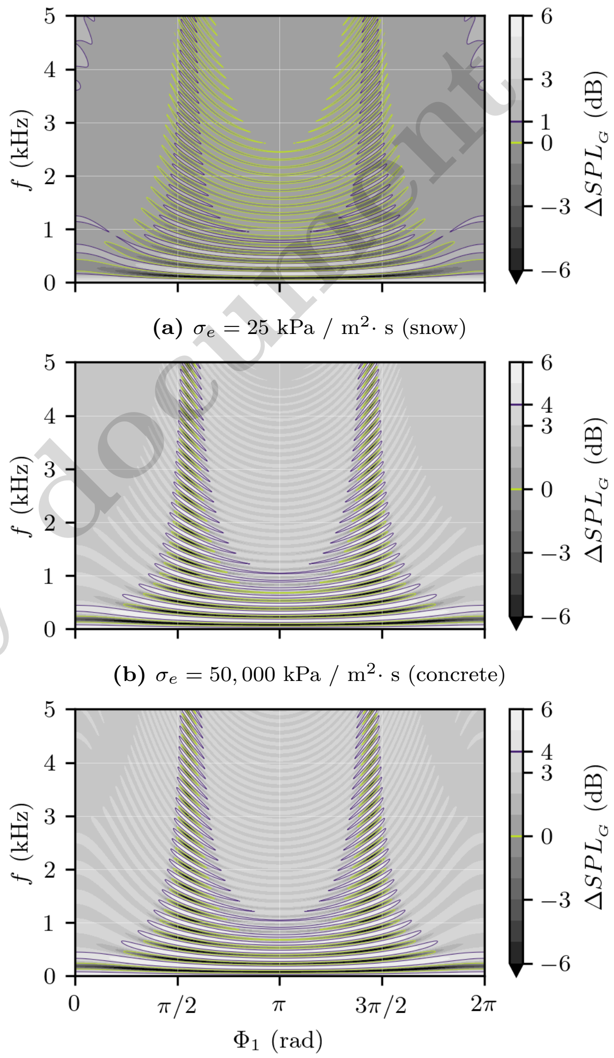

(a) $\sigma_e = 25$ kPa / m^2· s (snow)

(b) $\sigma_e = 50,000$ kPa / m^2· s (concrete)

(c) $\sigma_e = 10^7$ kPa / m^2· s (highly reflective surface)

Figure 8: Sensitivity of the ground reflection pattern to the ground material flow resistivity σ_e for three different ground materials ($N = 101$).

Regarding the number of point sources, Figure 9a shows that including too few sources results in aliasing bands with increased interference. Figure 9b furthermore shows these bands shift to higher frequencies as N increases, without significant changes to the remaining spectrogram. Figure 4, where $N = 1001$, shows no aliasing in the audible frequency ranges.

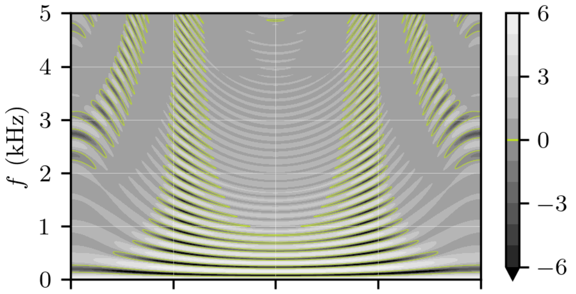

(a) $N = 11$

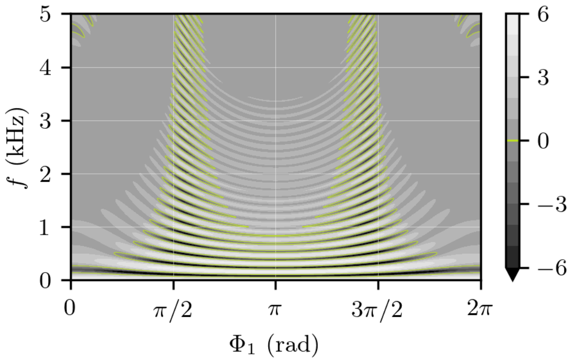

(b) $N = 21$

Figure 9: Sensitivity of the ground reflection pattern to the number of point sources N.

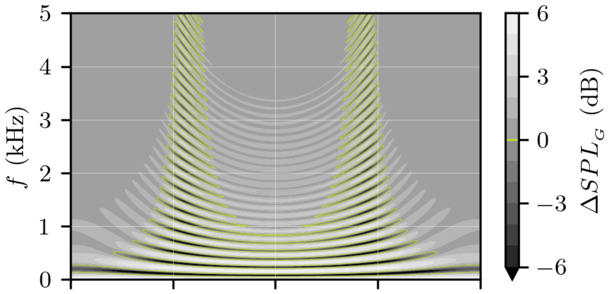

(a) Distributed point sources on each blade ($N = 101$).

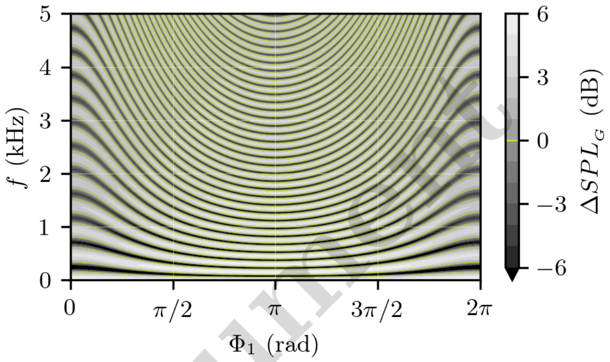

(b) Single point source at $r/R = 85\%$.

Figure 10: Comparison with point source assumption for a single blade.

The increased number of point sources results in a proportional increase in computational cost. This is an important result, as blade-element-based wind turbine noise prediction methods propagate noise from a limited number of point sources [14], which may inadvertently lead to aliasing if the number of sources is insufficient.

The geometry of the specific setup (wind turbine size and observer location) directly determines the wavelengths at which aliasing occurs. A mathematical description of the frequencies at which these aliasing bands occur will be explored in future work.

5. Comparison to point source models

Since propagation models for wind turbine noise commonly assume either a single static or three moving point sources, it is valuable to compare the method in this paper with the results from those assumptions.

Figure 10b shows the ground effect when a turbine blade is modelled as a single, moving point source at 85% of the rotor radius. As expected, using a single point source results in a more pronounced interference pattern over the full rotor rotation and across the full frequency range. Compared to the result in Figure 10a, modelling a blade as a single source results in a more prominent frequency response, with significant frequency modulation. Both factors will influence the human perception of modelled wind turbine noise. A similar result is observed for a three-bladed rotor in Figure 11b.

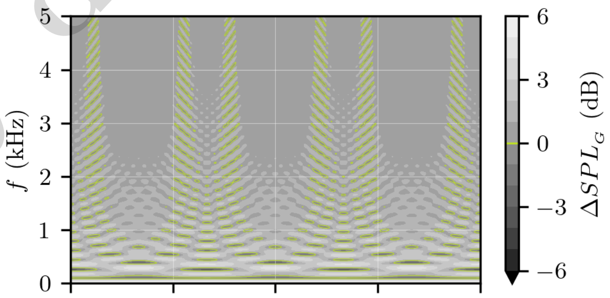

(a) Distributed point sources on each blade ($N = 3 \times 101$).

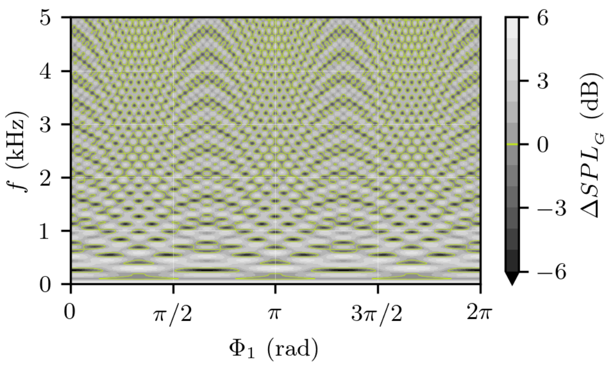

(b) Point source at $r/R = 85\%$, per blade.

Figure 11: Comparison with point source assumption for a three-bladed rotor.

In case a turbine is modelled using a singular point source at the rotor hub, the ground effect spectrum will be constant over time, with similar frequency content to a slice of Figure 10b. This assumption thus misses the frequency and amplitude fluctuations caused by the ground reflections.

6. Conclusion

A new method to determine the acoustic ground effect of a wind turbine was presented. The modelling approach consists of: (1) distributing the total source energy over multiple point sources per blade, (2) propagating the individual sources, and (3) incoherently summing the results. This method was applied to the NREL 5 MW reference wind turbine and a receiver located directly downstream at a height of 1.7 m. While the loss of phase coherence in a turbulent atmosphere was not fully modelled, it is shown to play a significant role in the ground-effect spectrograms.

For a single blade, in the geometry considered for this paper, acoustic interference was mostly limited to frequencies below 5 kHz. At higher frequencies, slight amplification remains nearly constant, except at two asymptotic blade positions. Increasing the ground material's flow resistivity σ_e increases the overall amplification and the acoustic interference. Using too few point sources results in undesired aliasing effects. A three-bladed rotor shows additional blade-to-blade interference, resulting in a complex pattern. Compared to a model with one moving point source per blade, the proposed method shows significantly less interference, especially at high frequencies.

Future work on the presented method will: (1) explore the effect of the turbulent atmosphere on the results, (2) verify it against experimental data, and (3) implement it in an auralisation toolchain to quantify its effect on human perception of modelled wind turbine noise.

7. Acknowledgments

This publication is part of the project *Listen to the future* (with project number 20247) of the research programme Veni 2022 (Domain Applied and Engineering Sciences), awarded to Roberto Merino-Martínez, which is (partly) financed by the Dutch Research Council (NWO).

References

[1] G. Costanzo and G. Brindley, "Wind energy in Europe - 2025 Statistics and the outlook for 2026-2030," Wind Europe, Brussels, Belgium, Tech. Rep., 2026.

[2] E. Koppen and K. Fowler, "International Legislation for Wind Turbine Noise," in *Proceedings of Euronoise 2015*, C. Glorieux, Ed., Maastricht, Netherlands, 2015, pp. 321–326.

[3] F. J. Müller et al., "Wind turbine noise annoyance – an interdisciplinary three-year field study," *Environment International*, vol. 202, p. 109 614, 2025. DOI: 10.1016/j.envint.2025.109614.

[4] Y. Tian and B. Cotté, "Modelling of ground and atmospheric effects on wind turbine noise," in *6th International Meeting on Wind Turbine Noise*, Glasgow, UK, 2015. [Online]. Available: https://ensta.hal.science/hal-01206965.

[5] J. S. Pockelé and R. Merino-Martinez, "Perceived Noise Impact of Transitioning Towards Larger Wind Turbines Using Auralisations," in *11th Edition of the International Conferences on Wind Turbine Noise: Conference Proceedings*, Copenhagen, Denmark, 2025. DOI: 10.11581/08042886-DEA0-4511-B4BD-6C5403125735.

[6] R. K. Amiet, "Noise due to turbulent flow past a trailing edge," *Journal of Sound and Vibration*, vol. 47, no. 3, pp. 387–393, 1976. DOI: 10.1016/0022-460X(76)90948-2.

[7] F. Brooks, D. S. Pope, and A. Marcolini, "Airfoil Self-Noise and Prediction," NASA Langley Research Center, Hampton, VA, USA, NASA Reference Publication 1218, 1989.

[8] J. D. Anderson, *Fundamentals of aerodynamics* (McGraw-Hill series in aeronautical and aerospace engineering), Sixth edition. New York, NY, USA: McGraw Hill Education, 2017, ISBN: 978-1-259-12991-9.

[9] T. F. W. Embleton, J. E. Piercy, and G. A. Daigle, "Effective flow resistivity of ground surfaces determined by acoustical measurements," *The Journal of the Acoustical Society of America*, vol. 74, no. 4, pp. 1239–1244, 1983. DOI: 10.1121/1.390029.

[10] M. Delany and E. Bazley, "Acoustical properties of fibrous absorbent materials," *Applied Acoustics*, vol. 3, no. 2, pp. 105–116, 1970. DOI: 10.1016/0003-682X(70)90031-9.

[11] J. Jonkman, S. Butterfield, W. Musial, and G. Scott, "Definition of a 5-MW Reference Wind Turbine for Offshore System Development," National Renewable Energy Laboratory (NREL), Golden, CO, USA, Tech. Rep. NREL/TP-500-38060, 947422, 2009. DOI: 10.2172/947422.

[12] R. Pieren and D. Lincke, "Auralization of aircraft flyovers with turbulence-induced coherence loss in ground effect," *The Journal of the Acoustical Society of America*, vol. 151, no. 4, pp. 2453–2460, 2022. DOI: 10.1121/10.0010121.

[13] International Electrotechnical Commission (IEC), "Wind turbines - Part 11: Acoustic noise measurement techniques," International Standard IEC 61400-11:2012, 2012.

[14] A. P. C. Bresciani, "Physical and perceptual prediction of wind turbine noise," Doctoral thesis, University of Twente, Twente, Netherlands, 2024. DOI: 10.3990/1.9789036559546.